DETERMINATION OF PHYSICAL AND STRUCTURAL-MECHANICAL CHARACTERISTICS OF EXPANDED CLAY CONCRETE

Ch.S. Raupov
Tashkent State Transport University, Candidate of Technical Sciences, Professor of the "Bridges and tunnels" Department
G.B. Malikov
Tashkent State Transport University, basic PhD student of the "Bridges and tunnels" Department

https://doi.org/10.5281/zenodo.7063765

Abstract. *The article presents the testing technique and the results of experimental studies of strength and deformation, as well as the structural and mechanical characteristics of structural expanded clay concrete of a dense structure under monotonous and low-cycle loading in compression and tension by a complex of physical methods (tensometric, ultrasonic pulsed and acoustic emission). Diagrams of deformation, the speed of passage of ultrasound and the number of acoustic pulses from the stress level are obtained. Empirical formulas are proposed for determining the boundaries of microcrack formation in expanded clay concrete.*

Keywords: *expanded clay concrete, compression, tension, monotonous and low-cycle loading, microcracking boundaries, complex of physical methods.*

ОПРЕДЕЛЕНИЕ ФИЗИЧЕСКИХ И СТРУКТУРНО-МЕХАНИЧЕСКИХ ХАРАКТЕРИСТИК КЕРАМЗИТОБЕТОНА

Аннотация. *В статье представлены методика испытаний и результаты экспериментальных исследований прочности и деформации, а также структурно-механических характеристик конструкционного керамзитобетона плотной структуры при монотонном и малоцикловом нагружении на сжатие и растяжение комплексом физических воздействий. методы (тензометрический, ультразвуковой импульсный и акустико-эмиссионный). Получены диаграммы деформации, скорости прохождения ультразвука и количества акустических импульсов от уровня напряжения. Предложены эмпирические формулы для определения границ образования микротрещин в керамзитобетоне.*

Ключевые слова: *керамзитобетон, сжатие, растяжение, монотонное и малоцикловое нагружение, границы микротрещин, комплекс физических методов.*

INTRODUCTION

The widespread use of local artificial porous aggregates instead of natural heavy aggregates in seismic regions of the Republic of Uzbekistan with a dry hot climate is a governing condition for increasing the efficiency of capital investments in the construction of transport and other important structures. A distinctive feature of expanded clay, which in terms of the production of lightweight concrete from porous aggregates, ranks first in comparison with other porous aggregates, is its relatively high strength at a relatively lower bulk density. The use of expanded clay concrete in bridge building instead of traditional concrete can significantly reduce the weight of structures, material consumption, transport and installation costs, and labor costs while maintaining the necessary strength, reliability, and durability of structures. It can improve performance, reduce loads on foundations, reduce the cost of bridge construction and, at the same time, and speed up their construction [1 – 7].

Theories of strength and fracture under compression and tension are of great importance for predicting the physical and mechanical characteristics of concrete, in particular the concepts of the boundaries of microcracking (R^o_{crc} and R^v_{crc}) [3, 8 – 15]. With these theories, it is possible to assess the kinetics of the process of microcracking in concrete and the safety margins of structures. The boundaries of microcracking and long-term compressive and tensile strength should be considered important characteristics of concrete to ensure reliable operation of the structure. The values of the boundaries of microcrack formation are quite important for describing the features of concrete behavior since they allow drawing a conclusion about the stage of the stress-strain state (SSS) [9].

An analysis of the results of studies on the boundaries of microcrack formation shows that these characteristics are ambiguously related to the compressive strength R_b and can vary significantly depending on the proportion of expanded clay concrete mix, the type and consumption of coarse aggregate and other factors [3, 8 – 14].

Particular attention is paid to the upper limit of microcrack formation since reaching this boundary indicates the transition to the third stage of the SSS, i.e., this indicates that microcracks merge into macrocracks, and divide the concrete structure into blocks. The blocks under load are displaced relative to each other, and this causes the destruction of the concrete matrix [9 – 12]. If the load level is close to the upper limit of microcracking, but does not exceed it, plastic strains under static loading stabilize over time (even under cyclic changes of loading [16, 17]). At present, the derivation of new formulas (more universal ones) applicable to concretes of different types and classes is relevant.

MATERIALS AND METHODS

Method for testing expanded clay concrete under monotonous and low-cycle loading and measuring instruments.

The composition of expanded clay concrete is given in table.1. Expanded clay gravel of two fractions 5–10 and 10–20 mm in a ratio of 40:60 was taken as a coarse aggregate produced in the Tashkent cement plant. As Portland cement, the cement of the Navoi cement plant was used, and the sand of the Tashkent quarry was used as quartz sand.

Table 1.

Composition of expanded clay concrete

Actual consumption of materials per m^3 of concrete	cement, kg	427
	sand, kg	629
	expanded clay, kg (l)	414 (727)
W/C (water/cement ratio)		0.49

Monotonic loading under compression and tension. Loading of specimens (prisms) of 70x70x280 mm and 150x150x600 mm dimensions and cylinders of 70 mm in diameter and 235 mm in height, made of expanded clay concrete under compression and tension, was performed according to the standard procedure on testing machines UMM-20 and P-250 with a maximum capacity of 200 and 2500 kN, respectively. Specimen loading was conducted in steps of no more than 0.1 of the expected breaking load with staying on the steps until the increase in short-term creep deformations ceased. The duration of staying on the steps under stepwise compression loading of specimens did not exceed 5 min.

Low-cycle loading under compression. Some specimens were tested under cyclic loading. Each step contained 1 cycle of loading and destruction. The duration of load staying at the upper and lower stress levels of a given step was determined by reaching such a shape of the deformation diagram, when, within the measurement accuracy, the hysteresis loop ceased to increase. This pattern of loading was realized up to a stress level not exceeding the upper limit of microcrack formation [18, 19].

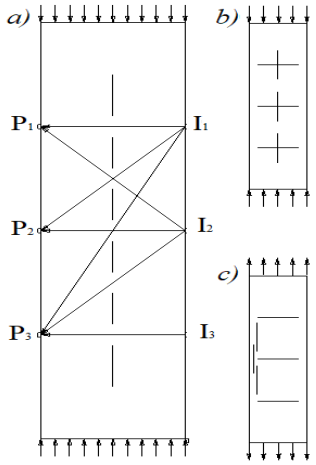

FIGURE 1. Scheme of ultrasonic and tensometric measurements

During short-term tests, longitudinal and transverse strains were measured with wiring strain paper gauges of with their own bases of 20 and 50 mm. To obtain information about the integral value of strains, longitudinal and transverse strains were measured in several sections along the length of the specimen, covering a certain volume of material [5].

The adopted pattern of strain gauge gluing is shown in Figures. 1 *a*, *b*, *c*. The dimensions of the tested prisms and the base of strain gauges determined the use of each pattern. Strain gauges were glued according to the standard method - three months before the start of the test. The scheme of installation of prisms and cylinders in a testing machine is shown in Figure 2.

Under compression tests, the specimens were centered along the physical axis by trial loading of no more than $0.20R_b$ (Figure 2, *a*). Under tensile testing, the load on the specimen was transferred through Hooke's hinges using collet grippers, which ensure uniform distribution of strain along the length of the specimen and reliable transfer of axial tensile force to the specimen. (Figure 2, *b*).

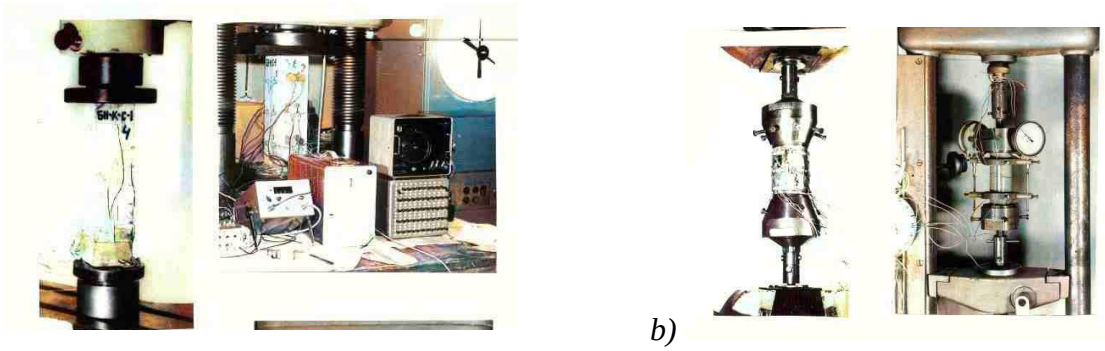

a) *b)*

FIGURE 2. Testing specimens under compression (a) and tension (b)

RESULTS

The results of determining the physical and structural-mechanical characteristics of expanded clay concrete under axial compression and tension.

Monotonic compression and tension loading. The strength and strain characteristics of expanded clay concrete under compression and tension are summarized in Tables 2 and 3.

Table 2.

The results of tests of expanded clay concrete for axial compression

Characteristics	Values, respectively, in age,

	days			
	28	220	530	800
Cubic strength of expanded clay concrete, *R*, MPa	33,0	36,5,	43,5	48,2
Prism strength, R_b, MPa	28,4	34,3	35,7	37,4
Prism strength factor, R_b/R	0,86	0,94	0,86	0,74
Modulus of elasticity, E_b, GPa	15,4	18,7	22,0	22,9
Poisson's ratio, ν_e		0,20	0,19	0,20
Compressibility at $0.95R_b$ $\varepsilon_{x(\sigma=0.95Rb)}.10^{-5}$		192	181	168
Bulk density of dry expanded clay concrete, kg/m^3	1760			

Note: *The results at the age of 28 and 800 days were obtained on prism samples with dimensions of 150x150x600 mm, cubes with an edge of 150 mm, and at the age of 220 and 530 days - 70x70x280 mm, cubes with an edge of 70 mm. The draft of the cone for the concrete mix was 1...2 cm.*

Table 3.

The results of tests of expanded clay concrete for axial tension

Characteristics	Values, respectively, in age, days	
	220	530
Tensile strength, R_{bt}, MPa	2,06	2,30
Modulus of elasticity, E_b, GPa	23,3	23,5
Poisson's ratio, ν_e	0,20	0,20
Tensile strength at $0.95R_{bt}$ $\varepsilon_{x(\sigma=0.95Rb)}.10^{-5}$	10	10

The data obtained (Table 2) on the increase in time of cubic *R* and prism R_b strength of expanded clay concrete confirmed that the measures we took to protect specimens from drying out during storage were sufficient and they provided a normal hardening condition for 800 days, which is very important when comparing the results of tests.

The increase in the elasticity modulus of expanded clay concrete under compression over time by the end of the experiment (τ_1= 800 days) was 30-50% higher than at the age of τ_1=28 days (Tables 2 and 3). The increase in the tensile modulus was less significant. So, by τ_1= 530 days, it increased only by 5% compared to τ_1= 220 days, while under compression over this time interval, the value of E_b increased by 15%.

For expanded clay concrete, the values of R_b/R exceed the ones specified in the existing standards for traditional concrete. Other researchers noted the increased prismatic strength of expanded clay concrete as well [1–5, 9–13]. They explained this by the fact that porous aggregates have a more developed surface and better adhesion with the cement-sand component, compared to dense aggregates. This largely restrains the transverse deformations of the prisms. However, with an increase in age, there was a noticeable decrease in the prism strength coefficient of expanded clay concrete and at the age of 800 days, R_b/R was 88% of R_b/R at 28 days of age (Table 2).

According to our experimental data, the coefficient of variation for the strength and strain properties of expanded clay concrete under compression and tension was 1–6% and 3–14%, respectively.

High values of the coefficients of variation under tension obtained in the experiments are due to two types of factors associated with the different nature of concrete destruction under compression and tension, respectively, and with different relative accuracy of measurements. Under axial tension, the destruction of the sample passes along one section, due to the presence of a local defect in the macrostructure. At that, as experiments have shown [5], there is practically no redistribution of stresses and strains between sections in concrete, and a weak section determines the strength of the entire sample.

Under compression, the effect of strain and stress localization is less pronounced due to their partial distribution over the entire volume of the specimen. The relative accuracy of measurements under compression and tension is due to the fact that the values of stress and strain measured during tensile testing are an order of magnitude less than under compression, while the resolution of force gauges and especially strain gauges is the same. This factor is especially pronounced when measuring tensile strains since the accuracy of their measurement, which does not exceed $1 \cdot 10^{-5}$, is commensurate with the measured strains, especially at low levels of loading.

The ratio of compressive and tensile strengths. The results of determining the axial tensile strength R_{bt} were compared with the results obtained for the cubic strength R and prism strength R_b (Tables 2 and 3).

In our experiments, the R_{bt}/R ratio was 0.05...0.06, and R_{bt}/R_b was 0.06...0.07. High ratio of R_{bt}/R for expanded clay concrete in our experiments is explained by the test procedure, where practical axial tension was ensured under the testing of cylinders. In addition, tensile tests of cylinders show better results compared to prisms, due to the smaller effect of friction in the corners of the specimen. The ratio of R_{bt}/R for expanded clay concrete can be approximately taken equal to 0.05.

Low-cycle compressive loading. The test results under low-cycle compressive loading are summarized in Table 4. A comparison of the data obtained with the data given in Tables 2 and 3, showed that low-cycle loading under compression had no effect on the strength of expanded clay concrete and mixes (the difference between the values of R_b did not exceed 6%).

Table 4.

Test results under low-cycle compressive loading

Prism strength R_b, MPa	The first	35.1
	The last	35.7
Modulus of elasticity Eb, GPa at the loading cycle	The first	19.7
	The last	19.0
Initial Poisson's ratio ν_e at the loading cycle	The first	0.21
	The last	0.22

The results obtained indicate the best resistance of expanded clay concrete under low-cycle compressive loading and the expediency of their use in transport engineering, where the structure are subject to multiple low-cycle loads. The values of Poisson's ratio ν_e practically did not change and did not differ from those obtained under monotonic loading. The elasticity modulus E_b of expanded clay concrete decreased by the last cycle by approximately 4%.

Determination of the boundaries of micro-crack formation in expanded clay concrete by a complex of physical methods

Tensometric method. Determination of R^{o}_{crc} and R^{v}_{crc} by tensometric methods based on the analysis of experimental *"η–ε"* diagrams was performed according to the method described in [15] by measuring longitudinal and transverse strains under loading.

Figures 3 and 4 show averaged diagrams of expanded clay concrete deformation obtained when testing specimens under compression and tension. Visually, general patterns of the deformation diagrams under axial compression and tension are similar. However, in the case of compression, the nonlinearity of the diagrams manifested itself earlier, and the degree of its curvature was greater than in the case of tension. A characteristic feature of all strain diagrams was an almost linear dependence between stresses and strains over a large part of the stress range. Inelastic strains were noted only at loading levels greater than 0.70.

Based on the measurement results, the average values of the longitudinal ε_x and transverse ε_y strains of the specimen were calculated, and, on their basis, volumetric strain ε_v, its increment $\Delta\varepsilon_v$, and the differential coefficient of transverse strain were determined at each stage of loading. The graphs of changes in these characteristics (Figure 3) were plotted depending on the relative level of loading. Five prisms were tested for expanded clay concrete. The values of mechanical characteristics (prism strength, modulus of elasticity, Poisson's ratio) were determined as an average of data for five specimens.

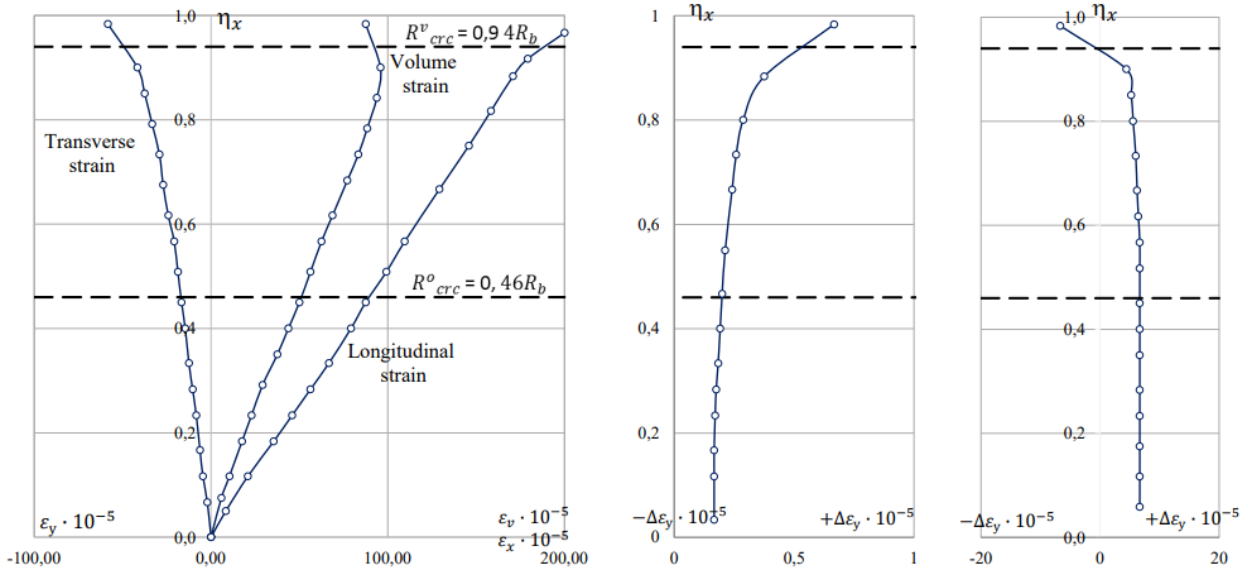

FIGURE 3. Strain of expanded clay concrete under axial compression (prism dimensions 70x70x280 mm)

A comparison of the strains determined by individual strain gauges on the specimen showed that the spread of their values was relatively small and changed little as the load increased. The coefficient of variation of readings from longitudinal strain gauges glued on different faces of the prism did not exceed 10%. This scatter was mainly due to the fact that the actual axis of load application did not coincide with the physical axis of the specimen. In a comparison of the readings from strain gauges located in different sections along the height on the same face, their coefficient of variation did not exceed 5%. Considering these results, the strains were determined as the arithmetic average values according to the readings of all strain gauges.

A comparison of the values of transverse strains, determined by individual strain gauges

on the specimen, showed that they were characterized not only by a higher spread (the coefficient of variation of their values was up to 40%), but by a sharp difference in the readings of individual strain gauges at individual points on the surface of the specimen (in the zone of potential destructions) almost from the beginning of loading.

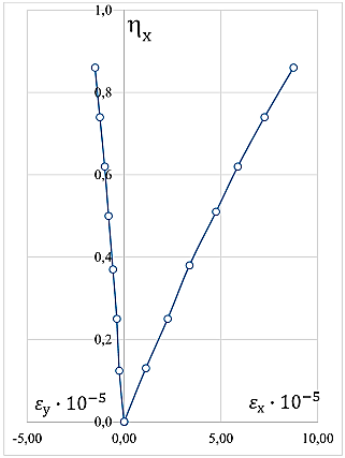

FIGURE 4. Strain of expanded clay concrete under axial tension

From experimental diagrams, strain values at 0.95 of breaking load were determined, since data on the compressibility and extensibility of concrete are used to solve a number of issues in the design and evaluation of research results. For expanded clay concrete and for heavy concrete, compressibility depends on a number of factors, of which the most important are the strength of concrete, the material of the aggregate, and the stress level of concrete [2, 6, 17].

Ultrasonic pulse method. The average diagrams of the change in the velocity of transmission of the generated ultrasonic pulses through the specimen are shown in Figures 5 and 6, and the results of determining R^0_{crc} are given in Table 5. Here, as well as in the case of the tensometric measurement method, the values of R^0_{crc}, determined from different scanning traces, can differ from each other by 20%.

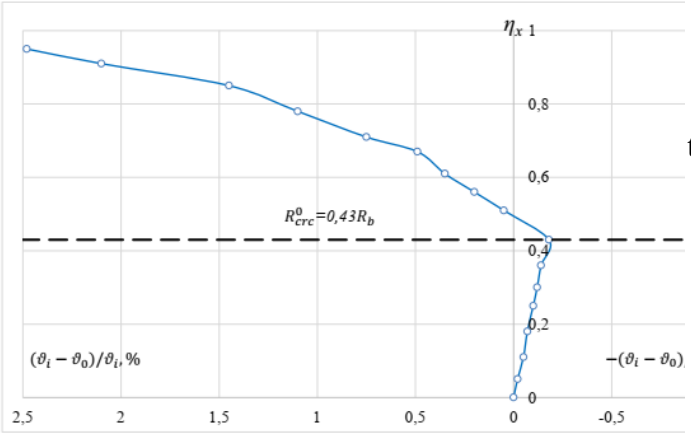

FIGURE 5. Diagram "velocity of ultrasound transmission vs stress level in expanded clay concrete specimens"

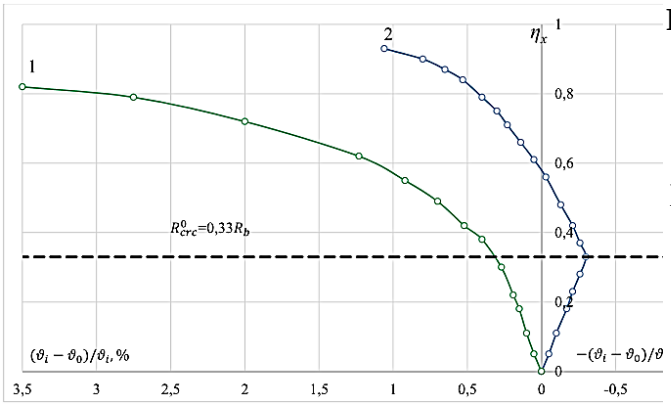

FIGURE 6. Diagram "velocity of ultrasound transmission vs stress level in expanded clay concrete specimens" at perpendicular (1) and diagonal (2) scanning

Acoustic emission method. The experiments conducted show (Figure 7) that the acoustic pulses accompanying the destruction of concrete structure are recorded almost from the moment of application of the compressive load and have several intensity peaks during the loading process. A point on the "$\eta - N$" diagram before the beginning of the first peak of the intensity of the growth of impulses N is taken as the lower boundary of microcracks, and a point before the last peak is taken as the upper boundary of microcracks. The first peak, apparently, corresponds to the microcrack development scheme proposed in [3, 15], to the formation of a system of microcracks originating from the initial cracks on the grains of the coarse aggregate. The next possible peaks should correspond to the formation of local systems of intergrown microcracks, and the subsequent peak should correspond to the formation of main macrocracks of destruction. The values of R^0_{crc}, obtained by the acoustic emission method (Table 5) are in good agreement with the values of R^v_{crc}, obtained by the tensometric method in the fracture zone (the discrepancy is no more than 8%).

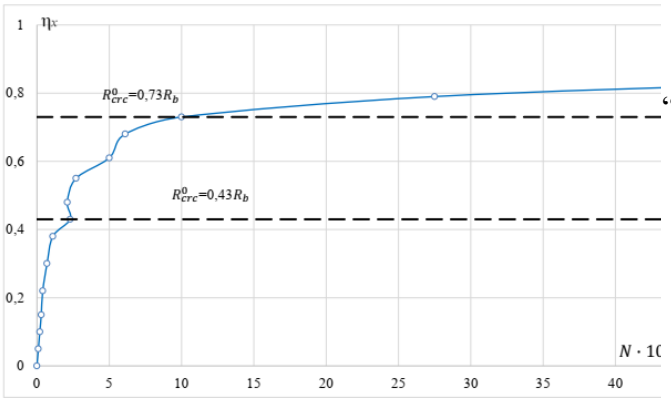

FIGURE 7. Diagram "number of acoustic pulses vs stress level in expanded clay concrete specimens"

DISCUSSION

The results of determining the boundaries of microcrack formation R^0_{crc}/R_b and R^v_{crc}/R_b by a complex of physical methods (strain gauge, ultrasonic pulse, and acoustic emission method) are given in Table 6.

Table 5.

Results of determining the boundaries of microcrack formation under compression by a complex of physical methods

Name of loading methods and types				Boundaries of microcrack formation		Values
Under compression	by the tensometric method (TM)	under cyclic loading	By average strains	R^v_{crc}/R_b		0.81
			By strains in the fracture zone	R^v_{crc}/R_b		0.75
			By maximum transverse and middle longitudinal strains	R^v_{crc}/R_b		0.35
		under monotonous loading	By average strains	R^0_{crc}/R_b		0.46
				R^v_{crc}/R_b		0.94
			By deformations in the fracture zone	R^0_{crc}/R_b		0.46
				R^v_{crc}/R_b		0.90
			By maximum transverse and	R^0_{crc}/R_b		0.23

			average longitudinal strains	R^{v}_{crc}/R_b		0.75
	By ultrasonic pulse method (UPM)			R^{0}_{crc}/R_b		0.43
	By acoustic emission method (AEM)			R^{0}_{crc}/R_b		0.43
				R^{v}_{crc}/R_b		0.73
By tensometric method for tension on average strains				R^{v}_{crc}/R_b		0.75

Note: *150x150x600 mm prism specimens were tested at the age of 800 days.*

The lower limit of microcrack formation R^{0}_{crc} of expanded clay concrete according to the tensometric method is weakly pronounced. It can be determined with a sufficiently large approximation only at the beginning of the increase in longitudinal and transverse strains (Figure 3) or with sufficient accuracy by the method of acoustic emission and ultrasound [15].

We similarly proposed as in [2] for high-strength expanded clay concrete of a dense structure, empirical formulas (1 and 2) are proposed. The values of the numerical coefficients are determined by the least squares method based on the experimental data of the authors

$$\eta^{o}_{crc} = R^{o}_{crc}/R_b = 0{,}21k_{crc} \times lnR_b - 0{,}11, \quad (1)$$

$$\eta^{v}_{crc} = R^{v}_{crc}/R_b = 0{,}21k_{crc} \times lnR_b + 0{,}21. \quad (2)$$

where R_b – the average strength of concrete, MPa; k_{crc} is the empirical coefficient.

Based on experimental data, it was determined that there is a linear relationship between the values of relative loads for the upper and lower limits of microcrack formation [20]. The ratio of the values of the load level corresponding to the lower boundary of microcracking to the value of the load level corresponding to the upper boundary remains constant regardless of the class of concrete, i.e. $\eta^{o}_{crc}/\eta^{v}_{crc}$= const.

The value of ratio $\eta^{o}_{crc}/\eta^{v}_{crc}$ can be taken [21]:

– $\eta^{o}_{crc}/\eta^{v}_{crc} \approx 0.67$ – for normal concrete;

–$\eta^{o}_{crc}/\eta^{v}_{crc} \approx 0.60$ – for expanded clay concrete;

The empirical coefficient k_{crc}, taken on the basis of value k_{c1}, can be used when performing calculations for concrete and reinforced concrete structures:

$$k_{crc} = k_{c1} \times \eta^{o}_{crc}/\eta^{v}_{crc} \quad (3)$$

where $k_{c1} \approx 1.2$ – for expanded clay concrete with concrete density ρ < 2200 kg/m^3, and for other types of concretes $k_{c1} = 1.0$ with ρ > 2200 kg/m^3.

The average values of R^{o}_{crc} and R^{v}_{crc} obtained by the authors in the experiment for expanded clay concrete were compared with those calculated using empirical formulas proposed by Semenyuk S.D., Moskalkova Yu.G. [16] and the authors (1 and 2) (Table 2).

Table 6.

Calculation results of relative values of microcrack boundaries

Concrete type	Average prism strength R_b, MPa	Relative values of microcrack formation boundaries			Deviations of calculated values from experimental ones, %	
		Test values	Experimental values		According to the methods of the authors	According to the method of Semenyuk S.D. and Moskalkova
			According to the formulas of the authors	Formulas [2]		

										Yu.G.	
		η_{crc}^{o}	η_{crc}^{v}	η_{crc}^{o}	η_{crc}^{v}	η_{crc}^{o}	η_{crc}^{v}	η_{crc}^{o}	η_{crc}^{v}	η_{crc}^{o}	η_{crc}^{v}
Normal concrete [16]	22,3	0,54	0,81	0,327	0,647	0,536	0,786	39,48	20,15	0,7	2,9
	28,1	0,53	0,83	0,359	0,679	0,588	0,838	32,20	18,15	-10,9	-0,9
	28,2	0,57	0,84	0,360	0,680	0,588	0,838	36,87	19,07	-3,2	0,2
	29	0,58	0,86	0,364	0,684	0,595	0,845	37,28	20,49	-2,5	1,8
Expanded clay concrete [8]	10,7	0,44	0,73	0,248	0,568	0,413	0,663	43,55	22,14	6,1	9,2
	11,2	0,44	0,73	0,255	0,575	0,424	0,674	41,98	21,19	3,6	7,7
	15,9	0,50	0,75	0,308	0,628	0,507	0,757	38,35	16,23	-1,5	-1,0
	17,7	0,45	0,75	0,324	0,644	0,533	0,783	27,89	14,07	-18,4	-4,4
Expanded clay concrete of dense structure	37,4	0.43	0,75	0,438	0,758	0,711	0,961	-1,77	-1,01	-65,23	-28,07

The data given in Table 4 clearly demonstrate the adequacy of the application of the empirical formulas proposed by the authors in (7, 8) to determine the relative values of the boundaries of microcracking in high-strength expanded clay concrete of a dense structure.

CONCLUSIONS

1. It was determined that the ratio of R_{bt}/R was 0.05...0.06, and R_{bt}/R_b - 0.06...0.07 and the values of the initial Poisson's ratio of expanded clay concrete under compression and tension correspond to the values regulated by building standards in regulatory documents.

2. The results obtained indicate the best resistance of expanded clay concrete under low-cycle compression loading and the expediency of their use in the structures of transport facilities, where the structures are subject to multiple low-cycle loads.

3. It was determined that the values of R_{crc}^{v}, calculated by different methods are in good agreement with each other, which cannot be said about R_{crc}^{o}. The values of R_{crc}^{v}, obtained by the acoustic emission method are in good agreement with the values of R_{crc}^{v}, obtained by the tensometric method in the fracture zone (the discrepancy is no more than 8%).

4. The statement is confirmed that for expanded clay concrete the values of relative levels of crack formation R_{crc}^{0}/R_b and R_{crc}^{v}/R_b are higher than for traditional heavy concrete of the same strength.

5. An empirical formula, convenient for practical application, has been obtained for determining the boundaries of microcracking (7, 8) of expanded clay concrete under axial compression. The results obtained allow the formulation of a number of proposals and clarifications for normative documents to calculate and design lightweight concrete elements and structures.

REFERENCES

1. Raupov, Ch., Shermukhamedov, U., & Karimova, A. (2021). Assessment of strength and deformation of lightweight concrete and its components under triaxial compression, taking into account the macrostructure of the material. In E3S Web of Conferences (Vol. 264, p. 02015). EDP Sciences.
2. Raupov, Ch., Karimova, A., Zokirov, F., & Khakimova, Y. (2021). Experimental and theoretical assessment of the long-term strength of lightweight concrete and its components under compression and tension, taking into account the macrostructure of the material. In E3S Web of Conferences (Vol. 264, p. 02024). EDP Sciences.
3. Raupov Ch.S. Expanded clay concrete for transport construction: Monograph / Tashkent: Tamaddun, 2020. – 356 p.
4. Raupov Ch.S., Umarov Kh.K. Recommended areas of application of expanded clay concrete in bridge building and its effectiveness. Bulletin of TashIIT. 2010 #1. P. 6 - 9.
5. Ashrabov A.A., Raupov Ch.S. Work of lightweight concrete beams in view of a descending branch of the diagram. International Conference held in Malaysia, the collection of scientific researches, 2002. Pp 139–142.
6. Ashrabov A.A., Raupov Ch.S. The normalization of long-lived durability of lightweight concrete at monoaxial stressing. International Conference held in Malaysia. The collection of scientific researches, 2002. Pp 134–138.
7. Raupov Ch.S. Technology for the manufacture of bridge structures from high-strength expanded clay concrete. Bulletin of TashIIT. 2008 No. 2. P. 11–15.
8. Farhad Ansari. Mechanism of microcrack formation in concrete / ACI Materials Journal, Vol. 86, Issue 5. Pp. 459–464.
9. Construction of unique buildings and structures, 2018, No. 7 (70) 24 Semenyuk S.D., Moskalkova Yu.G. Methods for determining the boundaries of microcrack formation // Construction of unique buildings and structures. 2018. No. 7(70). P. 22-30. DOI: 10.18720/CUBS.70.2
10. Chini A. R., Villavicencio E. J. Detection of Microcracks in Concrete Cured at Elevated Temperature / University of Florida, Gainesville, 2006. - 86 p.
11. Thomas T. C. Hsu. Fatigue and microcracking of concrete / Materials and Structures. Vol. 17, Issue 1. 1984. Pp 51–54.
12. Villavicencio, Camacho Enrique J. Analysis of Microcrack Behavior in Mass Concrete / University of Florida, 2006. –72 p.
13. A. Ashrabov, C. S. Raupov, A. A. A. Samad, J. Jayaprakash. Stady on force transfer mechanizm in cracked reinforced concrete elements. The International Conference on problems of mechanics and seismodynamics of structures. Proceedings. Tashkent. 27-28 May. 2004. Pp. 28–31.
14. A. A. Ashrabov, Y.V. Zaitsev, S. Spotar, C. S. Raupov. Modelling and strength simulation for concrete materials containing cracks. Tashkent. Journal of Problems of Mechanics. № 4, 2005. pp. 11–17.
15. Guchkin I.S. Study of the process of micro-destruction of expanded clay concrete under uniaxial compression by a complex of physical methods: Diss….Cand. Tech. Sci. - Penza: 1973. –150p.
16. Moskalkova Yu. G. Strength and deformability of bent reinforced concrete elements,

reinforced by the build-up of a compressed zone, under static and low-cycle loading: Diss. ... Cand. Tech. Sci.; 05.23.01; Belarusian-Russian University Mogilev, 2013. - 199 p.
17. Semenyuk S. D., Moskalkova Yu. G. Strength and deformability of bent reinforced concrete elements reinforced by the growth of a compressed zone under static and low-cycle loading: monograph. / Belarusian-Russian University Mogilev, 2017. -274 p.
18. Kalandarov K. Effect of cyclic loading on the work of eccentrically compressed reinforced concrete elements. //Thesis of the Diss…Cand. Tech. Sci. - Samarkand: 1994. –185p.
19. Khodzhaev A.A. Improving the calculation of reinforced concrete structures under regime loading. Diss…. Doctor of technical sciences. - Tashkent. 1997. - 437p.
20. Chini A. R., Villavicencio E. J. Detection of Microcracks in Concrete Cured at Elevated Temperature / University of Florida, Gainesville, 2006. 86 p.
21. Moskalkova Yu. H. Behavior of claydite at the stage of microcrack formation. Science and Construction. Kiev, 2017. No 3 (13). Pp. 40 – 43.
22. Raupov, Ch. S., Malikov, G. B., & Zokirov, J. J. (2022). The Method Of Testing Expanded Clay Concrete For Short-Term And Long-Term Compression And Tensile Testing And Measuring Instruments. Miasto Przyszłości, 25, 336-338.